Accepted by ApJ
Preprint typeset using LaTeX style emulateapj v. 6/22/04

arXiv:astro-ph/0604111v2 13 Apr 2006

HYPERVELOCITY STARS. I. THE SPECTROSCOPIC SURVEY

Warren R. Brown[1], Margaret J. Geller, Scott J. Kenyon, and Michael J. Kurtz
Smithsonian Astrophysical Observatory, 60 Garden St, Cambridge, MA 02138

Accepted by ApJ

ABSTRACT

We discuss our targeted search for hypervelocity stars (HVSs), stars traveling with velocities so extreme that dynamical ejection from a massive black hole is their only suggested origin. Our survey, now half complete, has successfully identified a total of four probable HVSs plus a number of other unusual objects. Here we report the most recently discovered two HVSs: SDSS J110557.45+093439.5 and possibly SDSS J113312.12+010824, traveling with Galactic rest-frame velocities at least $+508 \pm 12$ and $+418 \pm 10$ km s^{-1}, respectively. The other late B-type objects in our survey are consistent with a population of post-main sequence stars or blue stragglers in the Galactic halo, with mean metallicity $[\mathrm{Fe/H}]_{W_k} = -1.3$ and velocity dispersion 108 ± 5 km s^{-1}. Interestingly, the velocity distribution shows a tail of objects with large positive velocities that may be a mix of low-velocity HVSs and high-velocity runaway stars. Our survey also includes a number of DA white dwarfs with unusually red colors, possibly extremely low mass objects. Two of our objects are B supergiants in the Leo A dwarf, providing the first spectroscopic evidence for star formation in this dwarf galaxy within the last ∼30 Myr.

Subject headings: Galaxy: halo — Galaxy: stellar content — stars: horizontal-branch — (stars:) white dwarfs — galaxies: individual (Leo A, Draco)

1. INTRODUCTION

Hypervelocity stars (HVSs) travel with velocities so extreme that dynamical ejection from a massive black hole (MBH) is their only suggested origin. First predicted by Hills (1988), HVSs traveling ∼1,000 km s^{-1} are a natural consequence of a MBH in a dense stellar environment like that in the Galactic center. HVSs differ from runaway stars because 1) HVSs are unbound and 2) the classical supernova ejection (Blaauw 1961) and dynamical ejection (Poveda et al. 1967) mechanisms that explain runaway stars cannot produce ejection velocities larger than 200 - 300 km s^{-1} (Leonard 1991, 1993; Portegies Zwart 2000; Gualandris et al. 2004; Dray et al. 2005). Depending on the actual velocity distributions of HVSs and runaway stars, some HVSs ejected by the central MBH may overlap with runaway stars in radial velocity.

Following the original prediction of HVSs, Hills (1991) provided a comprehensive analysis of orbital parameters needed to produce HVSs, and Yu & Tremaine (2003) expanded the Hills (1988) analysis to include the case of a binary black hole and to predict HVS production rates. In 2005, Brown and collaborators reported the first discovery of a HVS: a $g' = 19.8$ B9 star, ∼110 kpc distant in the Galactic halo, traveling with a Galactic rest-frame velocity of at least $+709 \pm 12$ km s^{-1} (heliocentric radial velocity $+853$ km s^{-1}). Photometric follow-up revealed that the object is a slowly pulsating B main sequence star (Fuentes et al. 2006). Only interaction with a MBH can plausibly accelerate a 3 $M_\odot$ main sequence B star to such an extreme velocity.

The discovery of the first HVS inspired a wealth of theoretical and observational work. Because HVSs originate from a close encounter with a MBH, HVSs can be used as important tools for understanding the nature and environs of MBHs (Gualandris et al. 2005; Levin 2005; Ginsburg & Loeb 2006; Holley-Bockelmann et al. 2006; Demarque & Virani 2006). The trajectories of HVSs also provide unique probes of the shape and orientation of the Galaxy's dark matter halo (Gnedin et al. 2005). Recent discoveries of new HVSs (Edelmann et al. 2005; Hirsch et al. 2005; Brown et al. 2006) are starting to allow observers to place suggestive limits on the stellar mass function of HVSs, the origin of massive stars in the Galactic Center, and the history of stellar interactions with the MBH. Clearly, a larger sample of HVSs will be a rich source for further progress on these issues.

Here we discuss our targeted survey for HVSs and the unusual objects we find in it. To discover HVSs, we have undertaken a radial velocity survey of faint B-type stars, stars with lifetimes consistent with travel times from the Galactic center but which are not a normally expected stellar halo population. This strategy is successful: approximately 1-in-50 of our candidate B stars are HVSs. The first two HVS discoveries from our survey are presented in Brown et al. (2006). Here we present two further HVS discoveries – one certain HVS and one possible HVS. In addition to HVSs, our survey has uncovered many unusual objects with late B-type colors: post-main sequence stars, young B supergiant stars, DA, DB, and DZ white dwarfs, and one extreme low-metallicity starburst galaxy.

Our paper is organized as follows. In §2 we discuss the target selection and spectroscopic identifications of objects in our survey, now half complete. In §3 we present two new HVS discoveries. In §4 we show that the properties of the other late-B type stars in the sample are consistent with being a Galactic halo population of post-main sequence stars and/or blue stragglers. In §5 we discuss the white dwarfs in the sample, many of which may be unusually low mass DA white dwarfs. In §6 we discuss two young B supergiants in the Leo A dwarf galaxy and

---

Electronic address: wbrown@cfa.harvard.edu

[1] Clay Fellow, Harvard-Smithsonian Center for Astrophysics

one UV bright phase horizontal branch star in the Draco dwarf galaxy. We conclude in §7.

2. DATA

2.1. *Target Selection*

As Brown et al. (2006) discuss, HVSs ought to be rare: Yu & Tremaine (2003) predict there should be $\sim10^3$ HVSs in the entire Galaxy. Thus, in any search for HVSs, *survey volume is important.* Solar neighborhood surveys have not discovered HVSs because, even if they were perfectly complete to a depth of 1 kpc, there is only a $\sim$0.1% chance of finding a HVS in such a small volume. Finding a new HVS among the Galaxy's $\sim10^{11}$ stars also requires selection of targets with a high probability of being HVSs. Our observational strategy is two-fold. Because the density of stars in the Galactic halo drops off as approximately r^{-3}, and the density of HVSs drops off as r^{-2} (if they are produced at a constant rate), we target distant stars where we *maximize the contrast* between the density of HVSs and indigenous stars. Secondly, the stellar halo contains mostly old, late-type stars. Thus we target faint B-type stars, stars with lifetimes consistent with travel times from the Galactic center but which are not a normally expected stellar halo population. O-type stars are more luminous but do not live long enough to reach the halo. A-type stars are also luminous but must be detected against large numbers of evolved blue horizontal branch (BHB) stars in the halo. Based on the Brown et al. (2005b) field BHB luminosity function, we expect only small numbers of hot BHB stars with B-type colors. Our strategy of targeting B-type stars is further supported by observations showing that 90% of the $K < 16$ stars in the central 0.5″ of the Galactic Center are in fact normal main sequence B stars (Eisenhauer et al. 2005).

We use Sloan Digital Sky Survey (SDSS) photometry to select candidate B stars by color. Our color selection is illustrated in Fig. 1, a color-color diagram of stars with B- and A-type colors in the SDSS Fourth Data Release (Adelman-McCarthy et al. 2006). Fukugita et al. (1996) describe the SDSS filter system and the colors of main sequence stars in the SDSS photometric system. We use SDSS point-spread function magnitudes and reject any objects that have bad photometry flags. We compute de-reddened colors using extinction values obtained from Schlegel et al. (1998). The dotted box in Fig. 1 indicates the selection region used by Yanny et al. (2000) to identify BHB candidates. Interestingly, there is a faint group of stars with late B-type colors extending up the stellar sequence towards the ensemble of white dwarfs. We chose our primary candidate B star selection region inside the solid parallelogram defined by: $-0.38 < (g'-r')_0 < -0.28$ and $2.67(g'-r')_0 + 1.30 < (u'-g')_0 < 2.67(g'-r')_0 + 2.0$. In addition, we impose $-0.5 < (r'-i')_0 < 0$ to reject objects with non-stellar colors.

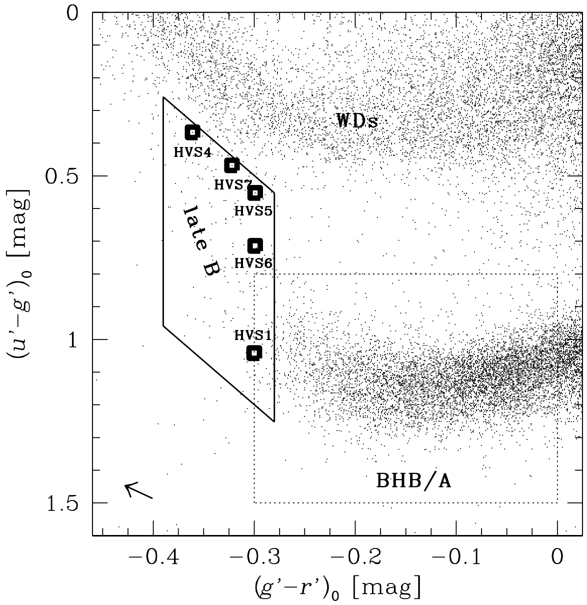

FIG. 1.— Color-color diagram showing our target selection, illustrated with every star in the SDSS DR4 $17.5 < g'_0 < 18.5$. For reference, BHB/A stars are located in the dotted box (Yanny et al. 2000). Candidate B-type stars extend up the stellar sequence towards the ensemble of white dwarfs, and are selected within the solid parallelogram. The arrow indicates the amplitude and direction of the median reddening correction for our targets. Open squares mark the HVSs we have discovered (Brown et al. 2005a, 2006) and the two new HVSs presented here.

We observe candidate B stars in the magnitude range $17.0 < g'_0 < 19.5$. The bright magnitude limit sets an inner distance boundary $\gtrsim$30 kpc for late B-type stars, a distance beyond that of known runaway B stars (Lynn et al. 2004; Martin 2004). We chose the faint magnitude limit to keep our exposure times below 30 minutes using the 6.5m MMT telescope. In addition, we exclude the region of sky between $b < -l/5 + 50°$ and $b > l/5 - 50°$ to avoid excessive contamination from Galactic bulge stars.

There are a total of 430 SDSS DR4 candidate B stars in the primary selection region described above. We have observed 192, or 45% of this total. The average surface number density of targets is 1 per 15 deg^2. Thus we have surveyed $\sim$3000 deg^2 or 7% of the entire sky. Figure 2 displays the locations of observed candidate B stars in the northern Galactic hemisphere; a handful of stars in the autumn SDSS equatorial stripes are located in the southern Galactic hemisphere and are not displayed.

In addition, we have observed 55 targets with colors, magnitudes, or positions slightly outside our primary selection region (for example, see Fig. 3). We include the full sample of 247 objects in our discussion below. We note that the region of sky located $40 < l < 90°$ in Fig. 2 lacks HVS discoveries, but this is probably not significant. This region, observed in July 2005, is missing observations of the bluest objects in $(u'-g')_0$ and will be completed in the coming months.

2.2. *Spectroscopic Observations and Radial Velocities*

Observations were obtained with the Blue Channel spectrograph on the 6.5m MMT telescope. Observations were obtained on the nights of 2005 July 10-11, 2005 December 3-5, and 2006 February 22-25. The spectrograph was operated with the 832 line/mm grating in second order, providing wavelength coverage 3650 Å to 4500 Å. Most spectra were obtained with 1.2 Å spectral resolution, however on one night of poor seeing we used a larger slit that provided 1.5 Å spectral resolution for 24 objects. Exposure times ranged from 5 to 30 minutes

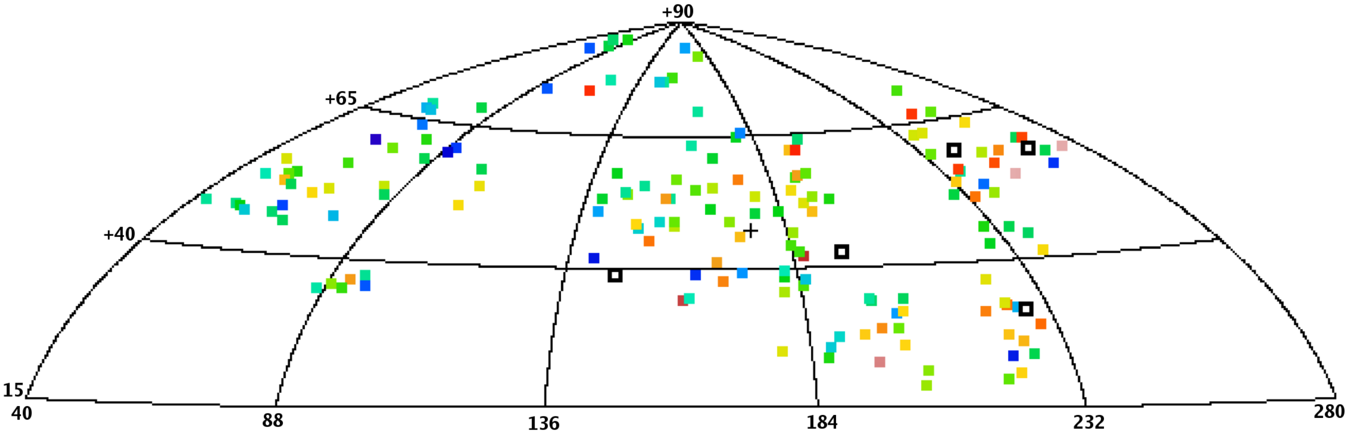

FIG. 2.— Aitoff sky map, in Galactic coordinates, showing the observed candidate B stars. Radial velocities, in the Galactic rest frame, are indicated by the color of the solid squares: purple is -300, green is 0, and red is +300 km s^{-1}. Our HVSs (see Table 1) are completely off this color scale and are marked by open squares; HVS2 (Hirsch et al. 2005) is marked by a plus sign.

and were chosen to yield $S/N = 15$ in the continuum at 4000 Å. Comparison lamp exposures were after obtained after every exposure.

Radial velocities were measured using the cross-correlation package RVSAO (Kurtz & Mink 1998). Brown et al. (2003) describe in detail the cross-correlation templates we use. Errors are measured from the width of the cross-correlation peak, and are added in quadrature with the 9 km s^{-1} systematic uncertainty observed in bright BHB standards. The average uncertainty is ±11 km s^{-1} for the late B-type stars and ±40 km s^{-1} for the DA white dwarfs (with much broader Balmer lines).

2.3. *Selection Efficiency and Unusual Objects*

Our candidate B stars include post-main sequence stars and late B blue stragglers, some DA white dwarfs, and a few other unusual objects. We classify the spectral types of the 202 late B stars based on O'Connell (1973) and Worthey et al. (1994) line indices as described in Brown et al. (2003). The spectral types of the stars range from B6 to A1 with an average uncertainty of ±1.6 spectral sub-types. Thus our primary target selection is 84% efficient for selecting stars of late B spectral type. Four of the 202 late B stars, or approximately 1-in-50, are HVSs. In addition, 3 of the late B stars coincide with Local Group dwarf galaxies, which provides special constraints on the nature of those objects.

Figure 3 plots the colors and spectroscopic identifications for the full sample of objects. The solid parallelogram indicates our primary color selection region; the dashed lines show the slightly different color selection regions used on different observing runs. 44 of the objects in Fig. 3 are white dwarfs marked by crosses. The white dwarfs are mostly DA white dwarfs, but also include one DB and one DZ white dwarf. Our sample also includes one extreme low-metallicity starburst galaxy, marked by the solid square in Fig. 3, that we describe in a separate paper (Kewley et al., in preparation).

3. HYPERVELOCITY STARS

Our targeted search for HVSs has discovered a total of four probable HVSs. Brown et al. (2006) report the discovery of the first two HVSs from this survey, and here we report two further HVS discoveries: SDSS J110557.45+093439.5 (hereafter HVS6) and possibly SDSS J113312.12+010824.9 (hereafter HVS7). HVS6 is a faint $g' = 19.06 \pm 0.02$ star with B9 spectral type and travels with a $+606 \pm 12$ km s^{-1} heliocentric radial velocity. HVS7 is a $g' = 17.75 \pm 0.02$ star with B7 spectral type and travels with a $+531 \pm 10$ km s^{-1} heliocentric radial velocity. We correct the velocities to the local standard of rest (Hogg et al. 2005) and remove the 220 km s^{-1}

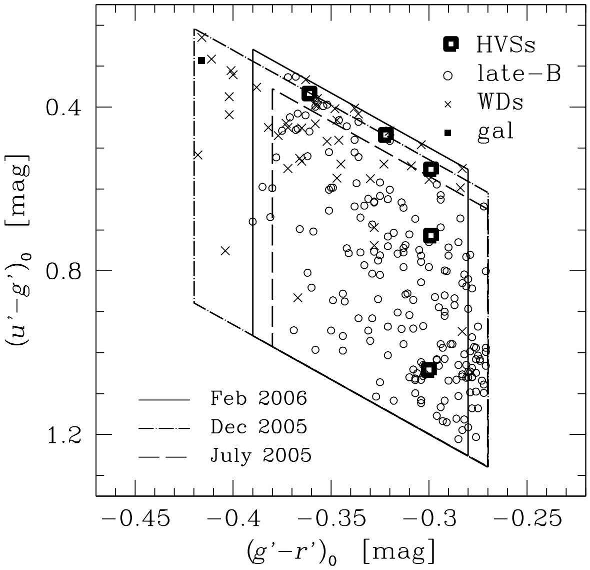

FIG. 3.— Color-color diagram showing spectroscopic identifications for the full sample of objects we observed with the MMT. The primary color-selection region is indicated by the solid line; dashed lines show the selection regions used during the December and July observing runs. The primary selection region is 84% efficient for selecting late B-type stars, of which approximately 1-in-50 are HVSs.

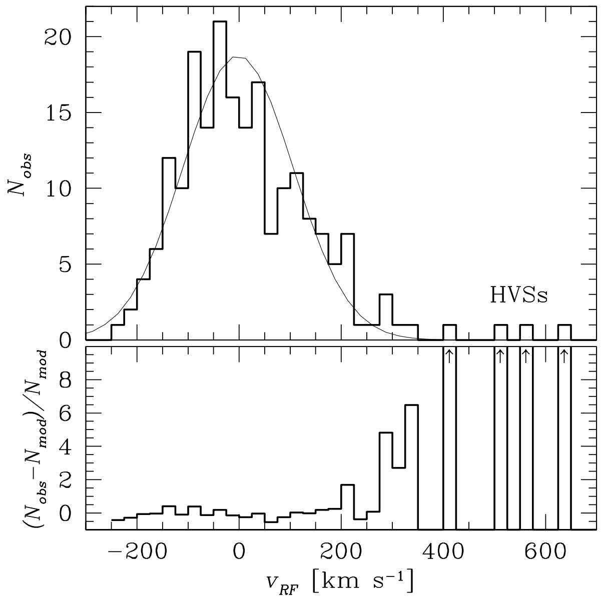

FIG. 4.— Galactic rest-frame velocity histogram of the late B-type stars (*upper panel*). The best-fit Gaussian (*thin line*) has dispersion 108 ± 5 km s^{-1}. Our survey has identified a total of four HVSs that are 4-6σ outliers from this distribution. The lower panel plots the residuals of the observations from the best-fit Gaussian, normalized by the value of the Gaussian. In addition to the HVSs, there is an interesting tail of high positive velocity objects $200 < v_{rf} < 400$ km s^{-1}.

solar reflex motion as follows:

$$v_{rf} = v_{helio} + (10\cos l \cos b + 5.2 \sin l \cos b + 7.2 \sin b) + 220 \sin l \cos b \quad (1)$$

The minimum Galactic rest frame velocities (indicated v_{rf}) of HVS6 and HVS7 are +508 and +418 km s^{-1}, respectively. The minimum Galactic rest-frame velocity of HVS7 is marginally consistent with runaway star mechanisms, but, if it is a main sequence B star, it is unbound to the Galaxy. Thus, for now, we consider HVS7 a HVS. All 7 known HVSs are traveling with large positive radial velocity, consistent with a Galactic center origin.

Figure 4 plots a histogram of Galactic rest-frame velocity for the 202 late B stars in our sample. We calculate the line-of-sight velocity dispersion of the stars using three different methods: 1) fitting a Gaussian to the entire distribution, 2) fitting a Gaussian to just the negative velocity half of the distribution, and 3) simply calculating the dispersion around the mean after clipping the HVSs. All three methods yield equivalent results. Averaging the results of the three methods, our sample has a velocity dispersion of 108 ± 5 km s^{-1} and mean of -2 ± 8 km s^{-1} consistent with a Galactic halo population.

HVS6 and HVS7 are 4.7σ and 3.9σ outliers, respectively, from the velocity distribution. The lower panel of Fig. 4 plots the residuals of the observations from the best-fit Gaussian, normalized by the value of the Gaussian. Stars with velocities below $|v_{rf}| < 200$ km s^{-1} show low-significance deviations from a Gaussian distribution. The four HVSs, on the other hand, are 4-6σ outliers and are completely off-scale.

In addition to the HVSs, the distribution of velocities in Fig. 4 shows a tail of stars traveling with large positive velocities $v_{rf} > 250$ km s^{-1} and no stars traveling with equally large negative velocities. Stars in compact binary systems may produce outliers in the velocity distribution, but such outliers should be distributed symmetrically. Conceivably, the observed asymmetry is the low-velocity tail of HVSs, or it may be the high-velocity tail of runaway stars. Because runaway stars are ejected with low < 300 km s^{-1} velocities, they follow bound, ballistic trajectories away from and then back onto the disk (e.g. Martin 2006). Thus, if the stars in the high velocity tail are runaway stars, they must be very nearby. The exact velocity distribution of runaway stars is, however, unclear. The predictions of Portegies Zwart (2000) are not applicable, for example, because the runaway stars must be low mass, intrinsically faint objects to be located nearby. Moreover, the velocity distribution of HVSs has been calculated for only restrictive sets of circumstances (Hills 1991; Levin 2005; Ginsburg & Loeb 2006). Clean predictions of runaway star and HVS velocity distributions are needed to discriminate among the populations in the high velocity tail. Proper motions (as may be measured with the *Hubble Space Telescope*, *GAIA*, or the *Space Interferometry Mission*) will ultimately discriminate between HVSs and runaway stars.

Our low-resolution spectra do not allow determination of exact stellar parameters for HVS6 and HVS7. Stars of late B spectral type are probably post-main sequence stars or main sequence B stars/blue stragglers. We note that the Balmer line widths of HVS6 and HVS7 are too broad to be consistent with those of luminosity class I or II B supergiants. If we assume the HVSs are BHB stars rather than B stars, their blue colors mean they are hot, extreme BHB stars and thus they are intrinsically very faint. The $M_V(BHB)$ relation of Clewley et al. (2002) yields $M_V(BHB) \simeq +1.6$ and +1.8 and heliocentric distance estimates $d_{BHB} \simeq$30 and 15 kpc for HVS6 and HVS7, respectively. In the BHB interpretation, the volume we effectively survey is much smaller than in the B star interpretation. Because the first two HVSs are known B stars (Edelmann et al. 2005; Fuentes et al. 2006) and because the B star interpretation implies a production rate probably consistent with Yu & Tremaine (2003), we assume that HVS6 and HVS7 are B stars for the purpose of discussion. The ultimate discriminant will come from higher resolution, higher signal-to-noise spectroscopy.

We estimate distances for HVS6 and HVS7 by looking at Schaller et al. (1992) stellar evolution tracks for 3 and 4 $M_\odot$ stars with $Z = 0.02$. A 3 $M_\odot$ star spends 350 Myr on the main sequence with $M_V(3M_\odot) \simeq -0.3$. If HVS6 is a 3 $M_\odot$ B9 main sequence star, it has a heliocentric distance $d \sim 75$ kpc. Using this distance, we now estimate the HVS travel time from the Galactic Center. We make the conservative assumptions that the HVS's observed velocity is a total space velocity and that its velocity has remained constant. Detailed calculations of HVS trajectories by Gnedin et al. (2005) show that this simple estimate is reasonably accurate and over-estimates HVS travel times by less than 10% (O. Gnedin, private communication). We estimate the travel time of HVS6 is $\sim$160 Myr, consistent with its 350 Myr main sequence lifetime. By comparison, a 4 $M_\odot$ star spends 160 Myr on the main sequence and has $M_V(4M_\odot) \simeq -0.9$. If HVS7 is a 4 $M_\odot$ B7 main sequence star, it has a heliocentric distance $d \sim 55$ kpc and a travel time from the Galactic center of ∼120 Myr also consistent with its lifetime. There is a tendency to find HVSs near the end of their lives because the longer they have traveled, the larger the survey volume they populate and the greater the contrast with the indigenous stellar populations.

Our radial velocities provide only a *lower* limit to the HVSs' true space velocities. The escape velocity from the Galaxy is approximately 300 km s^{-1} at 50 kpc (Wilkinson & Evans 1999), thus HVS6 is unbound to the Galaxy whether it is a B main sequence star or a BHB star. HVS7, on the other hand, is only unbound if it is a B main sequence star; follow-up spectroscopy is necessary to establish whether it is a "true" HVS.

HVS6 and HVS7 are both present in the USNOB1 (Monet et al. 2003) catalog but only HVS7 is listed with a proper motion. Averaging the USNOB1 proper motion with that from the GSC2.3 (B. McLean, 2006 private communication), HVS7 has $\mu = 10.5 \pm 9$ mas yr^{-1}. If we assume HVS7 is located nearby at $d_{BHB} \simeq 15$ kpc consistent with a proper motion detection, then its transverse velocity is 750 ± 650 km s^{-1}. Such a velocity would suggest that HVS7 is unbound, but the proper motion measurement is significant at only the 1σ level and thus we place little confidence in it.

The new HVSs are not physically associated with any other Local Group galaxy. HVS6 and HVS7 are located at $(l, b) = (243.^{\circ}1, 59.^{\circ}6)$ and $(263.^{\circ}8, 57.^{\circ}9)$, respectively (see Fig. 2). The nearest galaxies to HVS6 are Leo I and Leo II, both $\sim 14^{\circ}$ away on the sky from HVS6. However, Leo I and Leo II are at distances of 254 ± 17 kpc (Bellazzini et al. 2004) and 233 ± 15 (Bellazzini et al. 2005), respectively, many times the estimated distance of HVS6. Thus HVS6 is moving towards Leo I and Leo II at minimum velocities of 330 km s^{-1} and 490 km s^{-1}, respectively, and clearly unrelated to those galaxies. The nearest galaxy to HVS7 is the Sextans dwarf 20° away on the sky. At a distance of 1320 ± 40 kpc (Dolphin et al. 2003), Sextans is unrelated to HVS7.

Table 1 summarizes the properties of all seven known HVSs, four of which were discovered in this survey. The columns include HVS number, Galactic coordinates (l, b), apparent magnitude g', minimum Galactic rest-frame velocity v_{RF} (not a full space velocity), heliocentric distance estimate d, travel time estimate from the Galactic Center t_{GC}, and catalog identification. We have repeat observations of HVS1, HVS4, and HVS5; their radial velocities are constant within the uncertainties.

4. HALO STARS

Most objects in our survey are halo stars with late B spectral types, and we now discuss their nature. Stars of late B spectral type are probably main sequence stars / blue stragglers or post-main sequence stars. Unfortunately, main sequence stars and post-main sequence BHB stars share similar effective temperature (color) and surface gravity (spectral line widths), making classification difficult.

Stellar rotation is a useful discriminant between rapidly rotating main sequence B stars (Abt et al. 2002; Martin 2004) and slowly rotating BHB stars (Peterson et al. 1995; Behr 2003). However, our low-dispersion spectra do not allow us to measure rotation. Instead, we constrain the nature of the late B type objects by looking at their metallicities and kinematics.

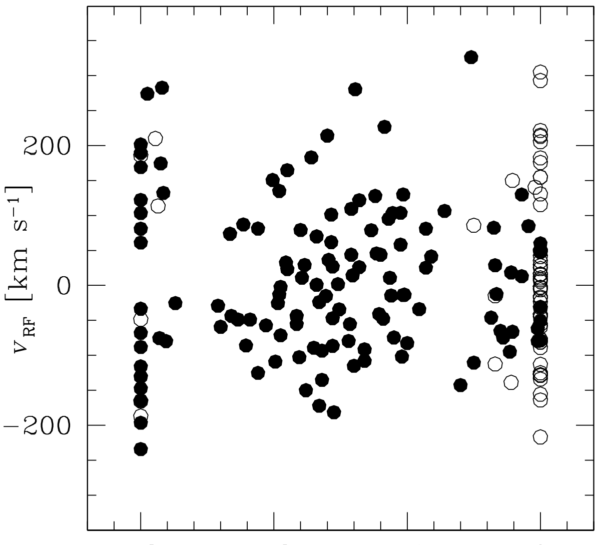

FIG. 5.— Metallicities and Galactic rest frame velocities of the late B stars. The Wilhelm et al. (1999) models restrict our metallicity estimates to $-3 < [\mathrm{Fe/H}]_{W_k} < 0$. These metallicities assume the stars have $\log g = 3$; using $\log g = 4$ does not substantially change the distribution. Hot objects with especially poor $[\mathrm{Fe/H}]_{W_k}$ determinations are plotted as open symbols.

The strongest indicator of metallicity in our spectra is the 3933 Å CaII K line. The equivalent width of CaII K depends on both temperature and metallicity. To estimate metallicity, we first compute $(B-V)_0$ from the SDSS colors following Clewley et al. (2005). We then measure the equivalent width of the CaII K line, W_k. Finally, we estimate metallicity $[\mathrm{Fe/H}]_{W_k}$ by interpolating the theoretical curves of Wilhelm et al. (1999), assuming $\log g = 3$ appropriate for a BHB star. We propagate the errors in $(B-V)_0$ and W_k through the Wilhelm et al. (1999) curves and find that the uncertainty is large, ± 0.67 in $[\mathrm{Fe/H}]_{W_k}$. Moreover, CaII K provides very little leverage on metallicity for the hottest stars $(B-V)_0 < -0.05$. For the 105 stars with $(B-V)_0 < -0.05$ our metallicity estimates are effectively reduced to a binary measurement: $[\mathrm{Fe/H}]_{W_k} \sim 0$ if we see CaII K, and $[\mathrm{Fe/H}]_{W_k} \sim -3$ if CaII K is absent. Note that the Wilhelm et al. (1999) models restrict our metallicity estimates to $-3 < [\mathrm{Fe/H}]_{W_k} < 0$.

Figure 5 plots metallicities and Galactic rest frame velocities of the late B type objects. We plot hot objects with poor $[\mathrm{Fe/H}]_{W_k}$ determinations as open symbols. All of the objects are affected at some level by accretion of interstellar material, atomic diffusion in their atmospheres, and observational effects such as interstellar absorption. We do not know the detailed histories of the individual stars, and thus we simply consider the average observed $[\mathrm{Fe/H}]_{W_k}$ of the sample. Ignoring the objects on the $[\mathrm{Fe/H}]_{W_k} = 0$ and -3 boundaries, it is clear that the objects cluster at metal-poor values: the mean metallicity of the sample (excluding objects on the boundaries) is $\overline{[\mathrm{Fe/H}]}_{W_k} = -1.3$. If instead we assume $\log g = 4$ appropriate for main sequence/blue straggler stars, additional stars are pushed onto the $[\mathrm{Fe/H}]_{W_k} = 0$ boundary line and the mean metallicity of the sample (excluding objects on the boundaries) increases slightly to $\overline{[\mathrm{Fe/H}]_{W_k}} = -1.2$. The low mean metallicity of the sample suggests that most objects are not recently-formed main sequence B stars ejected from the disk, but rather the objects are likely post-main sequence stars or old blue stragglers.

The observed 108 ± 5 km s^{-1} velocity dispersion of the late B type objects is also consistent with a Galactic halo population of post-main sequence stars or blue stragglers. Although some have proposed in-situ star formation in the halo (van Woerden 1993; Christodoulou et al. 1997), there is no evidence for this in modern studies of runaway B stars, including the recent Martin (2006) study of runaway stars in the Hipparcos catalog. Thus the observed metallicity and velocity distributions suggest that the late B type stars are most likely a Galactic halo population of post-main sequence stars and/or old blue stragglers, and not young runaway B stars ejected from the disk. We hope ultimately to use this sample to provide a useful probe of halo structure.

Table 2 lists the 202 spectroscopically identified late B type objects, including the 4 HVSs. The columns include RA and Dec coordinates (J2000), g' apparent magnitude, $(u'-g')_0$ and $(g'-r')_0$ color, and our heliocentric velocity v_{helio} and $[\mathrm{Fe/H}]_{W_k}$ estimate.

5. WHITE DWARFS

44 survey objects are faint white dwarfs, drawn from a largely unexplored region of color-space compared to previous SDSS-based white dwarf spectroscopic surveys (Harris et al. 2003; Kleinman et al. 2004; Kilic et al. 2006). The objects are almost entirely DA white dwarfs, with colors $-0.4 < (u' - g')_0 < 0.2$ indicating temperatures $10,000 < T_{eff} < 16,000$ K (Kleinman et al. 2004). Our color selection region, however, lies at surface gravities $\log g < 7$ for hydrogen-atmosphere white dwarfs (i.e. to the right of the Bergeron $\log g = 7$ curve plotted in Fig. 1 of Harris et al. (2003)). Thus the white dwarfs we find are all candidates for objects with unusually low surface gravities and unusually low masses.

The least massive white dwarfs known are $\sim$0.2 $M_\odot$ helium-core objects in binary systems containing millisecond pulsars (e.g. Callanan et al. 1998) or subluminous B (sdB) stars (Heber et al. 2003; O'Toole et al. 2006). Liebert et al. (2004) discuss a 0.18 $M_\odot$ helium white dwarf in the SDSS with colors $(u' - g') = 0.32$ and $(g' - r') = -0.35$ very similar to our white dwarfs (see Fig. 3). Figure 6 shows the spectra of two white dwarfs in our survey with the most unusually red $(u' - g')$ colors, SDSS J074508.15+182630.0 (top) and SDSS J083303.03+365906.3 (bottom). These objects do not appear to be sdB subdwarfs because their spectra show only very broad hydrogen Balmer lines. It would be very interesting to know whether these white dwarfs are unusually low mass white dwarfs, but detailed modeling is beyond the scope of this paper.

We search for proper motions in the USNOB1 and GSC2.3 catalogs, and find proper motion measurements for 35 of the 44 white dwarfs, 20 of which are significant at $> 3\sigma$ level. The average proper motion of the 20 white dwarfs is 40 mas yr^{-1} with an uncertainty of 7 mas yr^{-1}. The late B-type stars, by comparison, have no significant proper motion detections, consistent with their inferred distances. We calculate reduced proper motions for the white dwarfs with proper motion measurements and find values ranging $14 < H_{g'} < 18$ at $-0.7 < (g' - i')_0 < -0.5$, which places our objects in the main body of white dwarfs observed by Kleinman et al. (2004) and Kilic et al. (2006).

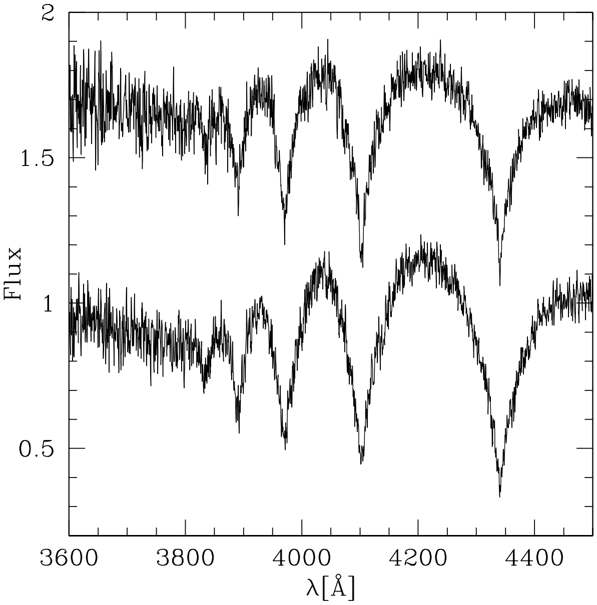

FIG. 6.— Spectra of two DA white dwarfs, SDSS J074508.15+182630.0 (*upper*) and SDSS J083303.03+365906.3 (*lower*), having unusually red $(u' - g')_0$ colors and possibly unusually low mass.

Table 3 lists the 44 spectroscopically identified white dwarfs. The columns include RA and Dec coordinates (J2000), g' apparent magnitude, $(u' - g')_0$ and $(g' - r')_0$ colors, and heliocentric radial velocities v_{helio}. We note that broad Balmer lines make for very poor radial velocity determinations. The objects are all DA white dwarfs with two exceptions: SDSS J111133.37+134639.8 is a DB white dwarf and SDSS J151852.49+530121.8 is a DZ white dwarf with strong calcium H and K lines.

6. UNUSUAL STARS IN DWARF GALAXIES

6.1. *B Supergiants in the Leo A Dwarf*

Leo A is an extremely metal-poor, gas-rich Im dwarf galaxy. Stellar population studies show that Leo A contains both very young and very old stellar populations (Tolstoy et al. 1998; Schulte-Ladbeck et al. 2002; Dolphin et al. 2002; Vansevičius et al. 2004). To date, stellar population studies of Leo A are based entirely on color-magnitude diagrams, all of which reveal a striking "blue plume" of B giants possibly in the galaxy. Here, we discuss the first spectroscopic identifications of two B giants definitely associated with the Leo A dwarf galaxy.

Two stars from our survey, SDSS J095915.12+304410.4 and SDSS J095920.22+304352.7, match Leo A both in position and in velocity. The stars are located 1.2′ and 2.0′, respectively, from the center of Leo A, well within the 7′ × 4.6′ Holmberg diameter of the galaxy (Mateo 1998). The stars have heliocentric radial velocity $+20 \pm$

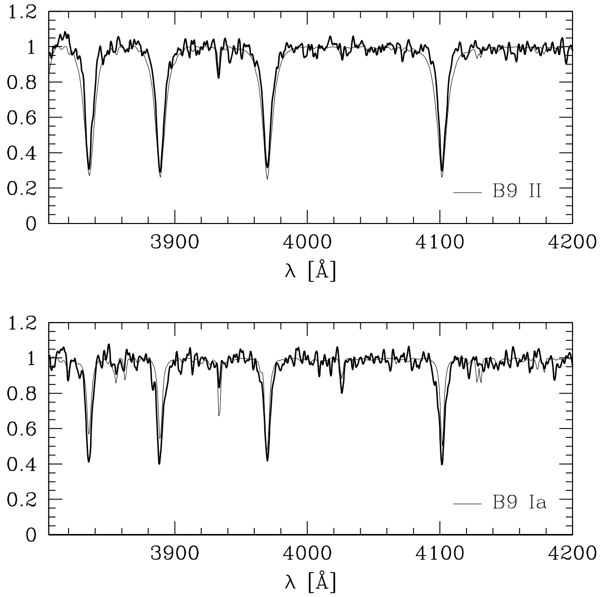

Fig. 7.— Spectra of SDSS J095915.12+304410.4 (*upper panel*) and SDSS J095920.22+304352.7 (*lower panel*) located in Leo A. The observations are convolved to match the 1.8 Å resolution of the B9 II and B9 Ia MK standards (Gray et al. 2003) overplotted as thin lines.

12 and +32±12 km s^{-1}, respectively, consistent at the 1σ level with the velocity of Leo A +24±2 km s^{-1} measured from 21 cm observations (Young & Lo 1996). The stars have apparent magnitude $g' = 19.90 \pm 0.03$ and 19.44 ± 0.03, respectively. If the stars are physically associated with Leo A, the galaxy's distance modulus $(m-M)_0 = 24.51 \pm 0.12$ (Dolphin et al. 2002) implies that the stars have luminosity $M_V \simeq -4.6$ and -5.0, respectively.

Interestingly, the spectra of the two stars in Leo A have unusually narrow Balmer lines for stars in our sample; cross correlation with MK spectral standards indicates that the stars are most likely luminosity class I or II B supergiants. Figure 7 displays a portion of the spectra for SDSS J095915.12+304410.4 (*upper panel*) and SDSS J095920.22+304352.7 (*lower panel*), convolved to match the 1.8 Å resolution of MK spectral standards from Gray et al. (2003). The B9 II (γ Lyr) and B9 Ia (HR1035) MK standards are over-plotted as thin lines. It is visually apparent that the observed stars have Balmer line widths between those of the B II and B Ia standards. Garrison (1984) give luminosities $M_V = -3.1$ for a B9 II star and $M_V = -5.5$ for a B9 Ib star. The luminosities we infer from the distance to Leo A fall between these values, consistent with the spectra. We conclude the two stars are B supergiants in the blue plume of the Leo A dwarf galaxy. Such stars are ∼30 Myr old (Schaller et al. 1992), consistent with star formation age estimates by others from color-magnitude diagrams.

6.2. *UV-Bright BHB Star in the Draco Dwarf*

By chance, another star from our survey is located in the Draco dwarf galaxy. The star, SDSS J172004.07+575110.8, has a spectral type of B9 and an apparent magnitude of $g' = 18.44 \pm 0.02$. The star is also identified as non-variable star #517 in the classic Baade & Swope (1961) paper. The distance modulus to Draco, $(m-M)_0 = 19.40 \pm 0.15$ (Bonanos et al. 2004), implies that the star has $M_V \sim -1$, a more difficult luminosity to explain. Unlike the two stars in Leo A, the star in Draco has Balmer line widths inconsistent with B giants. We conclude that the most likely explanation for the star in Draco is that it is a UV-bright, "slow blue phase" horizontal branch star.

The position, velocity, and metallicity of the star in Draco match that of the dwarf galaxy. The star falls within $5'$ of the center of the Draco, well within the $9'$ core radius of the galaxy (Irwin & Hatzidimitriou 1995). The star's velocity $v_{RF} = -82 \pm 12$ km s^{-1} is consistent at the 1σ level with the velocity of Draco -104 ± 21 km s^{-1} (Falco et al. 1999). Finally, our estimate of the star's metallicity, $[Fe/H]_{W_k} = -1.6 \pm 0.75$, is consistent with spectroscopic metallicity measurements of Draco's stellar population that fall into two groups near $[Fe/H] = -1.6 \pm 0.2$ and -2.3 ± 0.2 (Shetrone et al. 2001; Lehnert et al. 1992; Kinman et al. 1981; Zinn 1978).

The star in Draco is probably not a main sequence B star, because there is little evidence for young stars in color-magnitude diagrams of Draco (e.g. Bonanos et al. 2004; Klessen et al. 2003; Bellazzini et al. 2002). It is possible that a B9 main sequence star in Draco is a blue straggler. However, the luminosity of a metal-poor B9 main sequence star is too low to place it at the distance of Draco. A main sequence star with $Z = 0.001$ and $T_{eff} = 10,500$ K has a mass of 1.7 $M_\odot$ and an absolute magnitude $M_V(B9) = +1.6$ (Schaller et al. 1992), two-and-a-half magnitudes too faint to be at the distance of Draco.

The star in Draco is also unlikely to be a normal BHB star. The horizontal branch of Draco is well observed and its stars are $20 < V < 21$ (Klessen et al. 2003; Bellazzini et al. 2002). Moreover, a hot BHB star with spectral type B9 is an intrinsically faint star; the Clewley et al. (2004) $M_V(BHB)$ relation yields $M_V(BHB) = +1.3$ which is two magnitudes too faint to be at the distance Draco.

Other possibilities, such as a blue-loop Cepheid or a post-AGB star, are also unlikely. Cepheids with masses $> 5\ M_\odot$ can travel out of the instability strip on long blue loops (Bono et al. 2000), but massive stars are unlikely to exist in Draco. Post-AGB stars, stars in the process of blowing off their outer layers to become white dwarfs, can have effective temperatures of 10^4 K but only for a short time. Although there may be many more AGB stars than BHB stars in Draco, the substantially shorter $10^3 - 10^4$ yr timescale for a post-AGB star to have the correct effective temperature and luminosity (P. Demarque, private communication) suggests that a longer-lived, UV-bright star evolving off of the horizontal branch is a more plausible explanation.

The UV-bright phase is a slow-evolving, helium shell-burning phase that occurs for BHB stars with small hydrogen envelopes. Although the UV-bright phase is more common in metal-rich stars, it occurs in metal-poor stars as well. Yi, Demarque, & Kim (1997) stellar evolution tracks (see their Figure 1) show that metal-poor BHB stars with $\sim 0.05\ M_\odot$ envelopes spend 10^7 yrs at effective temperatures around 10,000 K and $10^{2.4}$ $L_\odot$. This model provides the exact absolute magnitude $M_V(UV\ BHB) = -1$ and spectral type needed to place the star at the distance of Draco, and applies to stars with metallicities ranging from [Fe/H]$= -1$ down to -2.6. A recent study of BHB stars in Draco identifies $\sim$50 BHB stars in the dwarf galaxy (Klessen et al. 2003). If BHB stars spend 150 Myr on the BHB and 10 Myr in the UV-bright phase, then we may expect a few BHB stars in the UV bright phase.

If the star in Draco is a UV-bright BHB star, its spectrum should indicate a low surface gravity. We estimate the surface gravity of the star by measuring the size and steepness of the Balmer jump (Kinman et al. 1994), and the widths and the shapes of the Balmer lines (Clewley et al. 2004). These independent techniques indicate that the star is a low surface gravity star. We conclude that the star in Draco SDSS J172004.1+575111 is most likely UV-bright BHB star.

7. CONCLUSIONS

In this paper we discuss our targeted survey for HVSs, a spectroscopic survey of stars with late B-type colors that is now half complete. Our survey has discovered a total of four HVSs, or approximately 1-in-50 of our candidates. The first two HVS discoveries are reported in Brown et al. (2006). Here we report two new HVS discoveries: HVS6 and possibly HVS7, traveling with Galactic rest-frame velocities at least $+508 \pm 12$ and $+418 \pm 10$ km s^{-1}, respectively. Assuming the HVSs are main sequence B stars, they are at distances $\sim$75 and $\sim$55 kpc, respectively, and have travel times from the Galactic center consistent with their lifetimes.

The remaining late B-type stars have metallicities and kinematics consistent with a Galactic halo population of post main-sequence stars or blue stragglers. However, the line-of-sight velocity distribution shows a tail of objects with large positive velocities. This high velocity tail may be a mix of low-velocity HVSs and high-velocity runaway stars; further theoretical and observational work is needed to understand the nature of the high velocity tail.

Our survey includes many interesting objects besides HVSs. Approximately one-sixth of the objects are DA white dwarfs with unusually red colors, possibly extremely low mass objects.

Two of our objects are luminosity class I or II B supergiants in the Leo A dwarf. Our observations of these B supergiants provide the first spectroscopic evidence for recent $\sim$30 Myr old star formation in Leo A. Another object is an unusual UV bright phase BHB star in the Draco dwarf.

We are continuing our targeted HVS survey of late B-type stars in the SDSS using the MMT telescope. We are also using the Whipple 1.5m telescope to obtain spectroscopy of brighter $15 < g' < 17$ late B-type objects. Given our current discovery rate, we expect to find perhaps another half dozen HVSs in the coming months. Follow-up high dispersion spectroscopy will provide precise stellar parameters of these stars, and *Hubble Space Telescope* observations will provide accurate proper motions. Our goal is to discover enough HVSs to allow us to place quantitative constraints on the stellar mass function of HVSs, the origin of massive stars in the Galactic Center, and the history of stellar interactions with the MBH.

We thank R. Zinn and P. DeMarque for helpful conversations, and the referee for a detailed report. We thank M. Alegria, J. McAfee, and A. Milone for their assistance with observations obtained at the MMT Observatory, a joint facility of the Smithsonian Institution and the University of Arizona. This project makes use of data products from the Sloan Digital Sky Survey, which is managed by the Astrophysical Research Consortium for the Participating Institutions. This work was supported by W. Brown's Clay Fellowship and the Smithsonian Institution.

Facilities: MMT (Blue Channel Spectrograph)

REFERENCES

Abt, H. A., Levato, H., & Grosso, M. 2002, ApJ, 573, 359
Adelman-McCarthy, J. K. et al. 2006, ApJS, 162, 38
Baade, W. & Swope, H. H. 1961, AJ, 66, 300
Behr, B. B. 2003, ApJS, 149, 67
Bellazzini, M., Ferraro, F. R., Origlia, L., Pancino, E., Monaco, L., & Oliva, E. 2002, AJ, 124, 3222
Bellazzini, M., Gennari, N., & Ferraro, F. R. 2005, MNRAS, 360, 185
Bellazzini, M., Gennari, N., Ferraro, F. R., & Sollima, A. 2004, MNRAS, 354, 708
Blaauw, A. 1961, Bull. Astron. Inst. Netherlands, 15, 265
Bonanos, A. Z., Stanek, K. Z., Szentgyorgyi, A. H., Sasselov, D. D., & Bakos, G. Á. 2004, AJ, 127, 861
Bono, G., Caputo, F., Cassisi, S., Marconi, M., Piersanti, L., & Tornambè, A. 2000, ApJ, 543, 955
Brown, W. R., Allende Prieto, C., Beers, T. C., Wilhelm, R., Geller, M. J., Kenyon, S. J., & Kurtz, M. J. 2003, AJ, 126, 1362
Brown, W. R., Geller, M. J., Kenyon, S. J., & Kurtz, M. J. 2005a, ApJ, 622, L33
—. 2006, ApJ, 640, L35
Brown, W. R., Geller, M. J., Kenyon, S. J., Kurtz, M. J., Allende Prieto, C., Beers, T. C., & Wilhelm, R. 2005b, AJ, 130, 1097
Callanan, P. J., Garnavich, P. M., & Koester, D. 1998, MNRAS, 298, 207
Christodoulou, D. M., Tohline, J. E., & Keenan, F. P. 1997, ApJ, 486, 810
Clewley, L., Warren, S. J., Hewett, P. C., Norris, J. E., & Evans, N. W. 2004, MNRAS, 352, 285
Clewley, L., Warren, S. J., Hewett, P. C., Norris, J. E., Peterson, R. C., & Evans, N. W. 2002, MNRAS, 337, 87
Clewley, L., Warren, S. J., Hewett, P. C., Norris, J. E., Wilkinson, M. I., & Evans, N. W. 2005, MNRAS, 362, 349
Demarque, P. & Virani, S. 2006, preprint (astro-ph/0603326)
Dolphin, A. E., Saha, A., Claver, J., Skillman, E. D., Cole, A. A., Gallagher, J. S., Tolstoy, E., Dohm-Palmer, R. C., & Mateo, M. 2002, AJ, 123, 3154
Dolphin, A. E., Saha, A., Skillman, E. D., Dohm-Palmer, R. C., Tolstoy, E., Cole, A. A., Gallagher, J. S., Hoessel, J. G., & Mateo, M. 2003, AJ, 125, 1261
Dray, L. M., Dale, J. E., Beer, M. E., Napiwotzki, R., & King, A. R. 2005, MNRAS, 364, 59
Edelmann, H., Napiwotzki, R., Heber, U., Christlieb, N., & Reimers, D. 2005, ApJ, 634, L181
Eisenhauer, F. et al. 2005, ApJ, 628, 246
Falco, E. E., Kurtz, M. J., Geller, M. J., Huchra, J. P., Peters, J., Berlind, P., Mink, D. J., Tokarz, S. P., & Elwell, B. 1999, PASP, 111, 438
Fuentes, C. I., Stanek, K. Z., Gaudi, B. S., McLeod, B. A., Bogdanov, S., Hartman, J. D., Hickox, R. C., & Holman, M. J. 2006, ApJ, 636, L37
Fukugita, M., Ichikawa, T., Gunn, J. E., Doi, M., Shimasaku, K., & Schneider, D. P. 1996, AJ, 111, 1748
Garrison, R. F., ed. 1984, The MK process and stellar classification (Toronto: DDO), 275
Ginsburg, I. & Loeb, A. 2006, preprint (astro-ph/0510574)
Gnedin, O. Y., Gould, A., Miralda-Escudé, J., & Zentner, A. R. 2005, ApJ, 634, 344

Gray, R. O., Corbally, C. J., Garrison, R. F., McFadden, M. T., & Robinson, P. E. 2003, AJ, 126, 2048

Gualandris, A., Portegies Zwart, S., & Eggleton, P. P. 2004, MNRAS, 350, 615

Gualandris, A., Zwart, S. P., & Sipior, M. S. 2005, MNRAS, 363, 223

Harris, H. C. et al. 2003, AJ, 126, 1023

Heber, U., Edelmann, H., Lisker, T., & Napiwotzki, R. 2003, A&A, 411, L477

Hills, J. G. 1988, Nature, 331, 687

—. 1991, AJ, 102, 704

Hirsch, H. A., Heber, U., O'Toole, S. J., & Bresolin, F. 2005, A&A, 444, L61

Hogg, D. W., Blanton, M. R., Roweis, S. T., & Johnston, K. V. 2005, ApJ, 629, 268

Holley-Bockelmann, K., Sigurdsson, S., Mihos, C. J., Feldmeier, J. J., Ciardullo, R., & McBride, C. 2006, preprint (astro-ph/0512344)

Irwin, M. & Hatzidimitriou, D. 1995, MNRAS, 277, 1354

Kilic, M. et al. 2006, AJ, 131, 582

Kinman, T. D., Kraft, R. P., & Suntzeff, N. B. 1981, in ASSL Vol. 88: Physical Processes in Red Giants, 71–76

Kinman, T. D., Suntzeff, N. B., & Kraft, R. P. 1994, AJ, 108, 1722

Kleinman, S. J. et al. 2004, ApJ, 607, 426

Klessen, R. S., Grebel, E. K., & Harbeck, D. 2003, ApJ, 589, 798

Kurtz, M. J. & Mink, D. J. 1998, PASP, 110, 934

Lehnert, M. D., Bell, R. A., Hesser, J. E., & Oke, J. B. 1992, ApJ, 395, 466

Leonard, P. J. T. 1991, AJ, 101, 562

Leonard, P. J. T. 1993, in ASP Conf. Ser. 45, Luminous High-Latitude Stars, ed. D. D. Sasselov, 360

Levin, Y. 2005, preprint (astro-ph/0508193)

Liebert, J., Bergeron, P., Eisenstein, D., Harris, H. C., Kleinman, S. J., Nitta, A., & Krzesinski, J. 2004, ApJ, 606, L147

Lynn, B. B., Keenan, F. P., Dufton, P. L., Saffer, R. A., Rolleston, W. R. J., & Smoker, J. V. 2004, MNRAS, 349, 821

Martin, J. C. 2004, AJ, 128, 2474

—. 2006, preprint (astro-ph/0603238)

Mateo, M. L. 1998, ARA&A, 36, 435

Monet, D. G. et al. 2003, AJ, 125, 984

O'Connell, W. O. R. 1973, AJ, 78, 1074

O'Toole, S. J., Napiwotzki, R., Heber, U., Drechsel, H., Frandsen, S., Grundahl, F., & Bruntt, H. 2006, Baltic Astronomy, 15, 61

Peterson, R. C., Rood, R. T., & Crocker, D. A. 1995, ApJ, 453, 214

Portegies Zwart, S. F. 2000, ApJ, 544, 437

Poveda, A., Ruiz, J., & Allen, C. 1967, Bol. Obs Tonantzintla Tacubaya, 4, 860

Schaller, G., Schaerer, D., Meynet, G., & Maeder, A. 1992, A&AS, 96, 269

Schlegel, D. J., Finkbeiner, D. P., & Davis, M. 1998, ApJ, 500, 525

Schulte-Ladbeck, R. E., Hopp, U., Drozdovsky, I. O., Greggio, L., & Crone, M. M. 2002, AJ, 124, 896

Shetrone, M. D., Côté, P., & Sargent, W. L. W. 2001, ApJ, 548, 592

Tolstoy, E. et al. 1998, AJ, 116, 1244

van Woerden, H. 1993, in ASP Conf. Ser. 45: Luminous High-Latitude Stars, ed. D. D. Sasselov, 11

Vansevičius, V. et al. 2004, ApJ, 611, L93

Wilhelm, R., Beers, T. C., & Gray, R. O. 1999, AJ, 117, 2308

Wilkinson, M. I. & Evans, N. W. 1999, MNRAS, 310, 645

Worthey, G., Faber, S. M., Gonzalez, J. J., & Burstein, D. 1994, ApJS, 94, 687

Yanny, B. et al. 2000, ApJ, 540, 825

Yi, S., Demarque, P., & Kim, Y.-C. 1997, ApJ, 482, 677

Young, L. M. & Lo, K. Y. 1996, ApJ, 462, 203

Yu, Q. & Tremaine, S. 2003, ApJ, 599, 1129

Zinn, R. 1978, ApJ, 225, 790

TABLE 1
HYPERVELOCITY STARS

ID	l deg	b deg	g' mag	v_{RF} km s^{-1}	d kpc	t_{GC} Myr	Catalog
HVS1	227.3	31.3	19.8	+709	110	160	SDSS J090745.0+024507[1]
HVS2	176.0	47.1	18.8	+717	19	32	US 708[2]
HVS3	263.0	-40.9	16.2	+548	61	100	HE 0437-5439[3]
HVS4	194.8	42.6	18.4	+563	75	130	SDSS J091301.0+305120[4]
HVS5	146.3	38.7	17.9	+643	55	90	SDSS J091759.5+672238[4]
HVS6	243.1	59.6	19.1	+508	75	160	SDSS J110557.45+093439.5
HVS7*	263.8	57.9	17.7	+418	55	120	SDSS J113312.12+010824.9

References. — (1) Brown et al. (2005a); (2) Hirsch et al. (2005); (3) Edelmann et al. (2005); (4) Brown et al. (2006)

Note. — HVS4 - HVS7 are from this targeted HVS survey.

*Probable HVS.

TABLE 2
LATE B OBJECTS

RA J2000	Dec J2000	g' mag	$(u'-g')_0$ mag	$(g'-r')_0$ mag	v_{helio} km s^{-1}	[Fe/H]$_{W_k}$
0:02:33.82	-9:57:06.8	18.578 ± 0.021	0.753 ± 0.040	-0.328 ± 0.040	-88 ± 10	0.0 ± 0.9
0:05:28.14	-11:00:10.1	19.271 ± 0.042	1.007 ± 0.081	-0.275 ± 0.047	-123 ± 12	-1.8 ± 1.0
0:07:52.01	-9:19:54.3	17.440 ± 0.017	1.016 ± 0.036	-0.276 ± 0.039	-119 ± 11	-1.6 ± 0.6

Note. — Table 2 is presented in its entirety in the electronic edition of the Astrophysical Journal. A portion is shown here for guidance and content.

TABLE 3
WHITE DWARFS

RA J2000	Dec J2000	g' mag	$(u'-g')_0$ mag	$(g'-r')_0$ mag	v_{helio} km s^{-1}
0:28:03.34	-0:12:13.4	18.414 ± 0.019	0.517 ± 0.032	-0.418 ± 0.025	97 ± 43
1:00:44.69	-0:50:34.1	20.111 ± 0.062	0.577 ± 0.097	-0.300 ± 0.068	73 ± 47
1:06:57.83	-10:08:39.3	19.417 ± 0.025	0.525 ± 0.072	-0.366 ± 0.035	-23 ± 47

Note. — Table 3 is presented in its entirety in the electronic edition of the Astrophysical Journal. A portion is shown here for guidance and content.